ELSEVIER

Computational Materials Science 22 (2001) 32–37

COMPUTATIONAL MATERIALS SCIENCE

www.elsevier.com/locate/commatsci

First-principles study of InP and GaP(0 0 1) surfaces

O. Pulci [a,*], K. Lüdge [b], P. Vogt [b], N. Esser [b], W.G. Schmidt [a], W. Richter [b], F. Bechstedt [a]

[a] *Institut für Festikörperphysik und Theoretische Optik, Friedrich-Schiller-Universität, Max-Wien Platz 1, D-07743 Jena, Germany*
[b] *Institut für Festkörperphysik, Technische Universität Berlin, Hardenbergstr. 36, D-10623 Berlin, Germany*

Accepted 2 April 2001

Abstract

The dependence of the GaP and InP(0 0 1) surface reconstructions on the chemical potentials of their constituents is explored. Based on *first-principles* pseudopotential plane-wave calculations the surface phase diagram is obtained. For both GaP(0 0 1) and Inp(0 0 1) surfaces, P-top dimer reconstructions are predicted for P-rich conditions, while for group III-element rich preparations a mixed dimer (III-P) on a complete III-layer is favoured. For GaP, in addition, a Ga-top dimer reconstruction seems to be a possibility for very Gallium rich growth conditions. STM images are calculated in order to contribute to a solution of the structural puzzle. © 2001 Published by Elsevier Science B.V.

1. Introduction

The understanding of the structure and composition of semiconductor surfaces during growth is one of the keys to control the evolution of epitaxial films on the atomic level, for instance using techniques like molecular beam epitaxy (MBE), chemical beam epitaxy (CBE) or metal-organic vapour-phase epitaxy (MOVPE). This holds in particular for the polar (0 0 1) surfaces of III–V semiconductors crystallizing in the zinc-blende structure. Their phases in dependence on substrate temperature and material fluxes, i.e., stoichiometry, have been studies experimentally in detail. On the InP(0 0 1) and GaP(0 0 1) surfaces several translational symmetries have been observed. For surfaces prepared under MBE, CBE and MOVPE conditions, reflection high-energy electron diffraction (RHEED) and low-energy electron diffraction (LEED) patterns with (2×2), (2×1), and (2×4) symmetry have been reported with increasing substrate temperatures and varying material fluxes [1–6]. Moreover, a weak $(c4 \times 4)$ for the InP(0 0 1) reconstruction has also been observed at lower temperatures [3,7]. Since P atoms desorb from the surface with increasing temperature, the surface becomes less P-rich. Consequently the (2×4) phase is know as "cation-rich", whereas lower temperature phases favour "P-rich" surfaces.

The present study aims to elucidate the atomic structure of the InP and GaP(0 0 1) surfaces in dependence on their preparation. A large variety of models representing (2×1), (2×2) and (2×4) translational symmetries is analysed. We perform *first-principles* total-energy (TE) calculations and construct the surface phase diagram. Furthermore,

* Corresponding author. Tel.: +49-3641-947168; fax: +49-3641-947152. Present address: Department of Physics, University of Rome Tor Vergata Via della Ricerca Scientifica 1, I-00133 Rome, Italy. Fax: +39-06-2023507.

E-mail addresses: pulci@ifto.physik.uni-jena.de, olivia.pulci@roma2.infn.it (O. Pulci).

0927-0256/01/$ - see front matter © 2001 Published by Elsevier Science B.V.
PII: S0927-0256(01)00161-6

experimental and calculated STM images for the GaP(0 0 1) Ga-rich surface are presented in order to clarify the structures.

2. Computational methods

The calculations are based on density-functional theory in the local-density approximation (DFT-LDA) [8,9]. A pseudopotential-plane-wave code is used [10,11]. The electron–ion interaction is treated by using fully separable, normconserving pseudopotentials [12]. The single-particle orbitals are expanded into plane waves up to an energy cut-off of 15 Ry for the InP, 18 Ry for the GaP surfaces. The **k**-space integrations are replaced a sum over eight special points in the irreducible part of the two-dimensional Brillouin zone (BZ) of the (2×2) phases and equivalent sets of points for the larger surface unit cells. Each unit cell includes an atomic slab with six to seven atomic layers and a vacuum region corresponding to five layers. The minima of the TE functional with respect to both the atomic and electronic degrees of freedom are found by means of a Car-Parrinello molecular-dynamical approach [13]. The calculations are performed with the theoretical equilibrium bulk lattice constant of 5.87 Å for InP, 5.42 Å for GaP.

The TE calculations are performed for a variety of structural models, shown in Fig. 1(a) for InP and in Fig. 1(b) for GaP, ranging from (2×4) to (2×1) and (2×2) reconstructions. As adlayers we consider mixed dimers (md) in parallel (p) or antiparallel (a) configurations, top-Gallium dimers (top-dim), buckled and unbuckled top-P dimers (td), possibly in a staggered arrangements (s), and phosphorous adatoms (aa).

The energetic comparison of the different structures is performed by calculating the phase diagrams [14,15]. We use the experimental value ΔH_f (InP) = 0.92 eV for the heat of formation of InP, and ΔH_f (GaP) = 0.91 eV for GaP [16]

3. Results

3.1. InP(0 0 1) surfaces

We have studied several geometries for the InP(0 0 1) surface, with different P coverages, as shown in Fig. 1(a).

For the intermediate P-rich growth conditions (P coverage between 0.5 and 1 ML) the structures are numbered from 2 to 7 in Fig. 1(a). The top-P dimer (td1) structures with the (2×1), (2×2) and $p(2 \times 2)$ translational symmetries are all not buckled. However, zig–zag chains observed by STM for intermediate P coverages [17,18], instead, suggest the presence of buckled dimers. In order to obtain zig–zag chains along the [1 1 0] direction we arranged phosphorous adatoms in an adlayer, shown as structure $c(2 \times 2)$aa1 (n. 4) in Fig. 1(a).

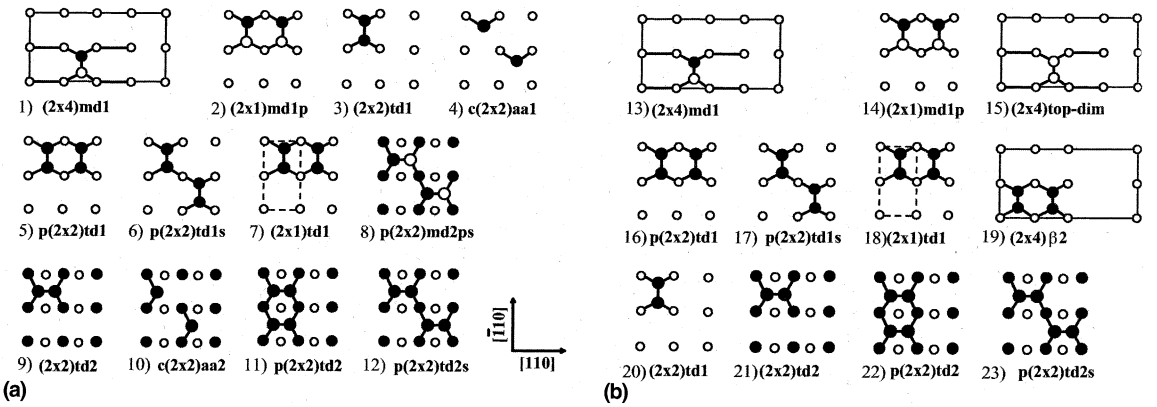

Fig. 1. Top view of the considered structures for InP(0 0 1) (a) and the GaP(0 0 1) (b) surface. Filled circles: P atoms; open circles: In, Ga atoms.

However, this adatom structure is unstable. If we instead allow the formations of dimers, i.e., the (2×2)td1 structure in Fig. 1(a), the energy decreases by about 0.3 eV per atom. The complete coverage of the In-terminated (0 0 1) surface by top-P dimer td1 with $p(2 \times 2)$td1 or $p(2 \times 2)$td1s translational symmetries offers further possibilities for the formation of chain structures. The two dimers per unit cell become inequivalent; for that reason no $c(2 \times 2)$ symmetry occurs in the staggered case. The two P dimers occur at different distances from the underlying In atomic layer, on the average about 2.2 Å. As a consequence of the inequivalence of the dimers, they might accomodate different numbers of electrons, and the surface may become semiconducting.

Another possibility to explain zig–zag chains along the [1 1 0] direction are mds of P and In atoms which are automatically buckled. We have considered several md overlayers on a In-layer with $c(2 \times 2)$ and $p(2 \times 2)$ periodicities. Among these md geometries, the energetically most favourable one is the md1p structure, consisting of two identical parallel In–P dimers per $p(2 \times 2)$ cell on an In layer and, hence, representing a 2×1 reconstruction. The dimer buckling amounts 0.48 Å, with the P atoms moving outwards and the In ones downward with respect to the surface plane. However, the resulting equal arrangement of P and In adatoms can only explain linear chains. Moreover, experimental findings from infrared spectroscopy rule out the possibility of In atoms on the top layer [17]. Also the observation of the dimer flipping seems to conclusively rule out mds [18]. In order to explain the obvious discrepancies between theory and experiment, at least for the $p(2 \times 2)$ translational symmetry observed in STM and assumed in the TE calculations, other reasons have to be considered, for instance a defect stabilization of local structures at real surfaces, adsorption of further species, such as hydrogen, or electron correlation effects.

For the more P-rich growth conditions the structures are numbered in Fig. 1(a) from 8 to 12. They are described by adatom arrangements, ranging from 1.5 to 2 ML of P and exhibiting a $p(2 \times 2)$ or $c(2 \times 2)$ translational symmetry. The (2×2)td2 structure (n. 9) has only one P dimer per 2×2 cell, on top of a complete P monolayer. It is buckled with a buckling amplitude of 0.69 Å. The driving forces for this reconstruction seem to be the same as in the case of Si and Ge(0 0 1) surfaces of bulk systems with a small energy gap [19]. A charge transfer from the lower to the upper P atom of the dimer occurs. The $c(2 \times 2)$aa2 structure with the same surface stoichiometry but without dimer bonds between the two extra P adatoms on top of the complete P monolayer is also unstable. This structure is about 0.1 eV/atom higher in energy than the (2×2)td2 one, thus showing that the dimer formation is always energetically more favourable. The two top-P dimer structures $p(2 \times 2)$td2 and $p(2 \times 2)$td2s with 2 ML of P show again no buckling. In contrast to the case of smaller coverage, e.g. 1.5 ML of P represented by the (2×2)td2, the dimer–dimer interaction makes buckling unfavourable. The semiconducting character of the surface is again a consequence of the geometrical and electronic inequivalence of the two dimers. As in the monolayer case, they differ with respect to the distance from the underlying complete P layer and with respect to their dimer lengths. These vertical and horizontal differences are 0.30 and 0.57 Å for the $p(2 \times 2)$td2 structure, and 0.64 and 1.00 Å for the $p(2 \times 2)$td2s one. We have also considered several md structures md2 with parallel and antiparallel arrangement of the dimers and $p(2 \times 2)$ translational symmetry. Among them, the energetically most favourable one is the $p(2 \times 2)$md2ps structure shown in Fig. 1(a), with a In–P buckling of about 0.6 Å.

Fig. 2(a) shows the surface energies Ω of the energetically most favourable InP(0 0 1) structures versus the In chemical potential in an interval slightly larger than the allowed range. The surface phase diagram of InP(0 0 1) also includes the (2×4) boundary of the In-rich phase. It is known [20–22] that under In-rich preparation conditions the (2×4) reconstruction is represented by a single md on top of the In-terminated surface (2×4mdl, n. 1 in Fig. 1(a)). The phase diagram shows that under more P-rich conditions (2×2) overlayer structures with two (n. 11 and 12) or 1.5 ML of P (n. 9) become more favourable. In the framework of the restriction to (2×2) translational symme-

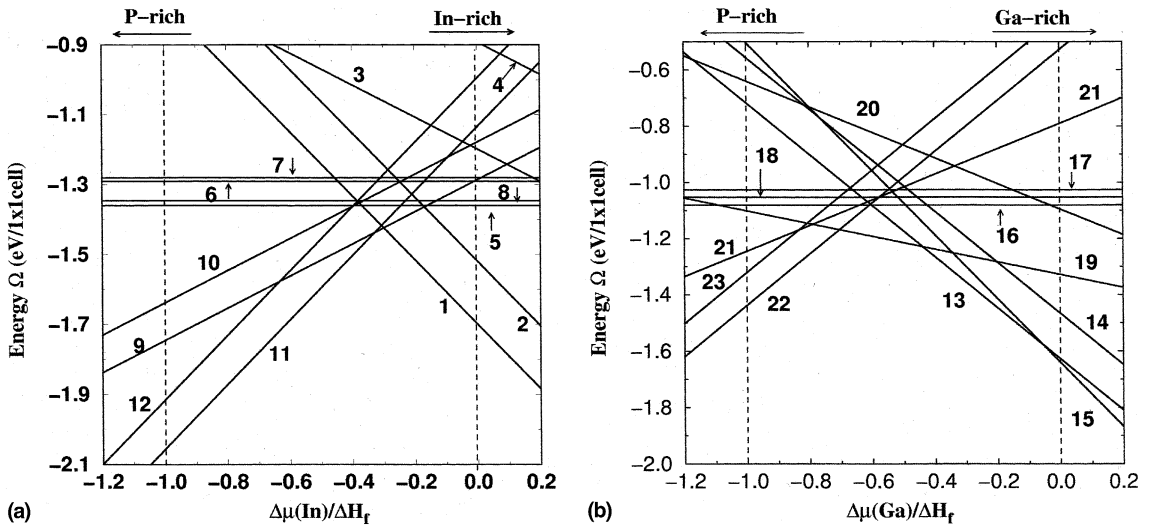

Fig. 2. Surface energy (with respect to the ideal unrelaxed P-terminated surface) per (1×1) unit cell versus the variation of the cation chemical potential, for InP(0 0 1) (a); for GaP(0 0 1) (b). Numbers refer to the structures shown in Figs. 1 (a) and (b).

tries several different surface geometries can be distinguished in dependence on the chemical potential of In. Under the most P-rich conditions the $p(2 \times 2)$td2 reconstruction (n. 11) is the energetically most favourable one. The staggered arrangement of the two P dimers, the $p(2 \times 2)$td2s structure (n. 12), is close in energy. Therefore its existence cannot be excluded. Defect-induced strain fields may stabilize other arrangements of the surface dimers. However, all favourable structures under P-rich conditions should contain two P monolayers with different P–P dimers in the uppermost atomic layer.

Vogt et al. [18] and Hicks et al. [23,24] observed for very P-rich growth conditions a mixture of domains of $c(4 \times 2)$, (2×2), and $c(2 \times 2)$ translational symmetry. However, a complete comparison of experimental and theoretical results is hardly possible [25]. On the one hand disorder effects obviously play an essential role. STM images indicate a random distribution of the local structures and many defects [18]. Hence, long-range order is absent, in contrast to the assumption in the TE calculations. Furthermore, in particular during the MOVPE growth of the P-rich InP(0 0 1) surfaces alkylgroups and H atoms may adsorb onto the P overlayer [23,24]. The adsorption onto half of the exposed phosphorous atoms in the uppermost layer probably would completely change the reconstruction behaviour.

3.2. GaP(0 0 1) surfaces

For the GaP(0 0 1) surfaces, the structural models shown in Fig. 1(b) have been studied. The stability of the investigated structures can be seen from the phase diagram in Fig. 2(b).

Similar to the InP(0 0 1) surfaces, under the extreme P-rich conditions the $p(2 \times 2)$td2 structure (n. 22 in Fig. 1(b)) is favourable in agreement with the experimentally observed translational symmetries [5,6]. This structure represents two complete monolayers of phosphorous. The atoms in the uppermost atomic layer are dimerized. The dimers are arranged in linear chains parallel to the $[\bar{1}\,1\,0]$ direction. Compared to the zig–zag chain arrangement in the $p(2 \times 2)$td2s structure (23 in Fig. 1(b)) an energy of about 0.1 eV per surface atom is gained. Our calculations show no evidence for dimer buckling [26].

Under Ga-rich conditions two structures, the (2×4)md1 and (2×4)top-dim (number 13 and 15, respectively, in Fig. 1(b)) are found to be stable, in agreement with previous results [5]. In the case of the GaP(1 0 0) (2×4) top-Ga-dimer, the Ga–Ga dimer bond length is 2.47 Å, slightly

smaller than the sum of the covalent radii (2.52 Å). The Ga–P dimer of the (2×4) md structure, with a bond length of 2.36 Å, shows a buckling with an angle of 9.51° (that is, the P atom is 0.39 Å above the Ga one). Since both structures are stable for Ga rich conditions, further experimental evidence was needed. Therefore STM images were taken. In Fig. 3(a) the STM image of a Ga-rich GaP(0 0 1) surface (grown by MOVPE and annealed at 450°C [27]) is shown. The image was taken at a sample bias of −3.5 V, thus only filled states contribute. A row-like structure in the $[\bar{1}\,1\,0]$ direction is clearly seen. A triangular-like structure along the rows is well resolved within this image. The single triangles are separated by 8.1 Å, corresponding to a twofold lattice constant. In order to interpret the experimental STM images, we performed ab initio calculations of the electron density to simulate STM mages. We use the Tersoff–Haman approach [28]. In order to take into account the extent of a real tip, we integrate the local electron density in space between 1 and 3 Å above the surface. Depending on the number of energy bands that is summed up, STM images corresponding to different voltages (applied to the sample with respect to the tip) can be simulated.

In Figs. 3(b) and (c) the simulated STM images of both the md (2×4)md1 and the top-Ga-dimer (2×4)top-dim reconstruction on GaP(1 0 0) are shown, for an energy interval of 2.3 eV below the VBM, in order to simulate the experimental voltage of −3.5 V. The simulated filled state STM images of the md (2×4) GaP surface (Fig. 3(b)), show rows in the $[\bar{1}\,1\,0]$ direction containing a triangular structure that repeats every two surface lattice constants. This triangular structure is rather independent of the voltage assumed. The reason is, that in any case we include the most important surface states in the integration. The more intensive circle like spot of this structure is formed by the dangling bonds at the P atom of the mds. This dangling bond is filled with two electrons. It is the highest occupied band, thus it can be seen also at very small voltages. The more faint spots of the structure are given by filled backbonds between the Ga atom in the md and neighbouring Ga atoms in the atomic layer beneath. In contrast, the simulated filled state STM images of the top-Ga-dimer reconstruction (Fig. 3(c)) contain a symmetric X-pattern that is visible within the rows. Also this pattern turns out to be rather independent of the energy below the Fermi level (e.g. voltage). The X-shape behaviour is a consequence of the backbonds between the Ga atoms in the top dimers and the Ga atoms beneath. Comparing the filled-states results to the measured STM images described above, the similarities between the simulated md STM images and the experimental data

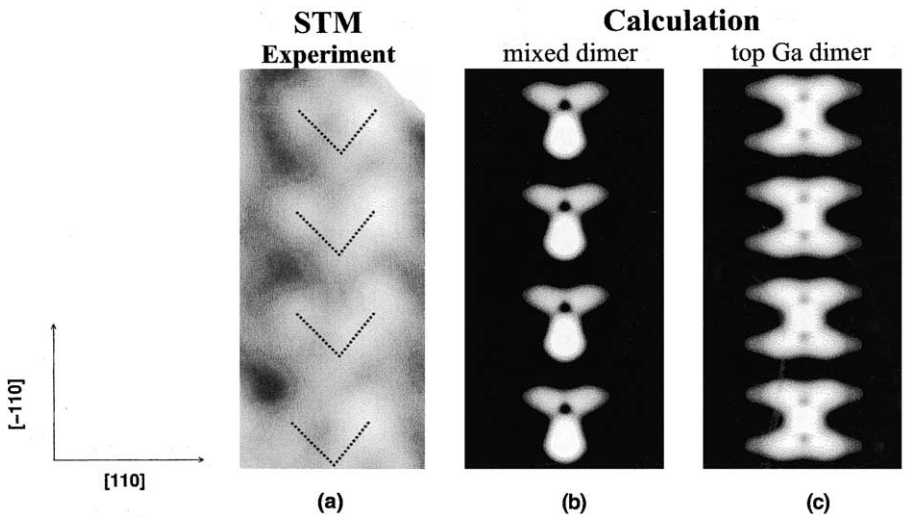

Fig. 3. Experimental and calculated STM image for the (2×4) Ga-rich GaP(0 0 1) surface.

lead to the conclusion, that the observed (2×4) reconstruction is the md structure (2×4)md1 (n. 13).

4. Conclusions

We have presented a comprehensive study of the structure as well as energetics and the accompanying ab initio thermodynamics of the reconstructed polar (0 0 1) surfaces of InP and GaP for different growth conditions. Under P-rich conditions the surface reconstructions are governed by P–P dimers.

Under cation-rich conditions (2×4 reconstruction) a md on top of a complete cation layer is favourable. The comparison of the experimental and calculated STM images shows that the energetically possible GaP(0 0 1) 2×4 top-Gallium dimer is still not observed. It may require more Ga-rich growth conditions.

Acknowledgements

This work was financially supported by the Deutsche Forschungsgemeinschaft (Contracts No. Be 1346/10-1 and ES127/4-2). The calculations have been done using the computer facilities of the J.V. Neumann Institut Jülich.

References

[1] B.X. Yang, H. Hasegawa, Jpn. J. Appl. Phys. 33 (1994) 742.
[2] B. Junno, S. Jeppesen, M.S. Miller, L. Samuelson, J. Cryst. Growth 164 (1996) 66.
[3] K.B. Ozanyan, P.J. Parbrook, M. Hopkinson, C.R. Whitchouse, Z. Sobiesierski, D.I. Westwood, J. Appl. Phys. 82 (1997) 474.
[4] M. Zorn, B. Junno, T. Trepk, S. Bose, L. Samuelson, J.-T. Zettler, W. Richter, Phys. Rev. B 60 (1999) 11597.
[5] A.M. Frisch, W.G. Schmidt, J. Bernholc, M. Pristovsek, N. Esser, W. Richter, Phys. Rev. B 60 (1999) 2488.
[6] N. Esser, W.G. Schmidt, J. Bernholc, A.M. Frisch, P. Vogt, M. Zorn, M. Pristovsek, W. Richter, F. Bechstedt, Th. Hannappel, S. Visbeck, J. Vac. Sci. Technol. B 17 (1999) 1691.
[7] M. Zorn, T. Trepk, J.-T. Zettler, B. Junno, C. Meyne, K. Knorr, T. Wethkamp, M. Klein, M. Miller, W. Richter, L. Samuelson, Appl. Phys. A: Mater. Sci. Process. 65 (1997) 333.
[8] P. Hohenberg, W. Kohn, Phys. Rev. 136 (1964) B864.
[9] W. Kohn, L.J. Sham, Phys. Rev. 140 (1965) A1133.
[10] R. Stumpf, M. Scheffler, Comput. Phys. Commun. 79 (1994) 447.
[11] M. Bockstedte, A. Kley, J. Neugebauer, M. Scheffler, Comput. Phys. Commun. 107 (1997) 187.
[12] D.R. Hamann, Phys. Rev. B 40 (1989) 2980.
[13] R. Car, M. Parrinello, Phys. Rev. Lett. 55 (1985) 2471.
[14] G.-X. Qian, R.M. Martin, D.J. Chadi, Phys. Rev. Lett. 60 (1988) 162.
[15] G.-X. Qian, R.M. Martin, D.J. Chadi, Phys. Rev. B 38 (1988) 7649.
[16] D.R. Lide (Ed.), CRC Handbook of Chemistry and Physics, 77th ed., CRC Press, Boca Raton, FL, 1996.
[17] L. Li, B.-K. Han, Q. Fu, R.F. Hicks, Phys. Rev. Lett. 82 (1999) 1879.
[18] P. Vogt, Th. Hannappel, S. Visbeck, K. Knorr, N. Esser, W. Richter, Phys. Rev. B 60 (1999) R5117.
[19] H. Krüger, J. Pollmann, Phys. Rev. Lett. 74 (1995) 1155.
[20] W.G. Schmidt, F. Bechstedt, N. Esser, M. Pristovsek, Ch. Schultz, W. Richter, Phys. Rev. B 57 (1998) 14596.
[21] W.G. Schmidt, F. Bechstedt, Surf. Sci. 409 (1998) 474.
[22] W.G. Schmidt, E.L. Briggs, J. Bernholc, F. Bechstedt, Phys. Rev. B 59 (1999) 2234.
[23] L. Li, B.-K. Han, C.H. Li, Q. Fu, R.F. Hicks, Appl. Phys. Lett. 75 (1999) 683.
[24] L. Li, Q. Fu, C.H. Li, B.-K. Han, R.F. Hicks, Phys. Rev. B 61 (2000) 10223.
[25] O. Pulci, K. Lüdge, W.G. Schmidt, F. Bechstedt, Surf. Sci. 464 (2000) 272.
[26] O. Pulci, W.G. Schmidt, F. Bechstedt, Phys. Stat. Sol., 184 (2001) 105.
[27] K. Lüdge, P. Vogt, O. Pulci, N. Esser, F. Bechstedt, W. Richter, Phys. Rev. B 62 (2000) 11046.
[28] J. Tersoff, D.R. Hamann, Phys. Rev. B 31 (1985) 805.